

# Catch Planner: Catching High-Speed Targets in the Flight

Huan Yu<sup>\*,1,2,3</sup>, Pengqin Wang<sup>\*,4</sup>, Jin Wang<sup>†,1,2,3</sup>, Jialin Ji<sup>5,6</sup>, Zhi Zheng<sup>1,2,3</sup>, Jie Tu<sup>1,2,3</sup>,  
Guodong Lu<sup>1,2,3</sup>, Jun Meng<sup>3,7</sup>, Meixin Zhu<sup>8</sup>, Shaojie Shen<sup>4</sup> and Fei Gao<sup>†,5,6</sup>

**Abstract**—Catching high-speed targets in the flight is a complex and typical highly dynamic task. In this paper, we propose Catch Planner, a planning-with-decision scheme for catching. For sequential decision making, we propose a policy search method based on deep reinforcement learning. In order to make catching adaptive and flexible, we propose a trajectory optimization method to jointly optimize the highly coupled catching time and terminal state while considering the dynamic feasibility and safety. We also propose a flexible constraint transcription method to catch targets at any reasonable attitude and terminal position bias. The proposed Catch Planner provides a new paradigm for the combination of learning and planning and is integrated on the quadrotor designed by ourselves, which runs at 100hz on the onboard computer. Extensive experiments are carried out in real and simulated scenes to verify the robustness of the proposed method and its expansibility when facing a variety of high-speed flying targets.

**Index Terms**—Motion Planning, Decision Making, Spatio-Temporal Trajectory Optimization, Deep Reinforcement Learning, Catching.

## I. INTRODUCTION

**A**UTONOMOUS aerial robots, thanks to its high maneuverability, can be employed for many highly complex and dynamic tasks such as aerial interception [2], aerial perching [3], task dispatching [4], juggling [5], racing [6], etc.. Catching is the most complex and typical problem among all the highly dynamic tasks, which requires not only accurate target motion prediction and precise interception but also adaptability and flexibility in the catching moment. In addition, it is necessary to make decisions of catching time and sequence when facing multiple targets. For catching task, motion planning and decision making (planning-with-decision) is the most important

This work was supported in part by the National Natural Science Foundation of China under Grant 52175032, the Key R&D Program of Zhejiang Province under Grant2021C01065 and 2020C01026, and Robotics Institute of Zhejiang University under Grant K12107 and K11805.

<sup>1</sup>The State Key Laboratory of Fluid Power and Mechatronic Systems, School of Mechanical Engineering, Zhejiang University, Hangzhou 310027, China. <sup>2</sup>the Engineering Research Center for Design Engineering and Digital Twin of Zhejiang Province, School of Mechanical Engineering, Zhejiang University, Hangzhou 310027, China. <sup>3</sup>Robotics Institute of Zhejiang University, Hangzhou 310027, China. <sup>4</sup>The Hong Kong University of Science and Technology (HKUST). <sup>5</sup>The State Key Laboratory of Industrial Control Technology, College of Control Science and Engineering, Zhejiang University, Hangzhou 310027, China. <sup>6</sup>Huzhou Institute of Zhejiang University, Huzhou 313000, China. <sup>7</sup>School of Electrical Engineering, Zhejiang University, Hangzhou 310027, China. <sup>8</sup>The Hong Kong University of Science and Technology (Guangzhou).

Email: {h.yu, dwjcom}@zju.edu.cn

<sup>†</sup>Corresponding author: Jin Wang, Fei Gao.

\*These authors contributed to the work equally.



Fig. 1: The process of the quadrotor catching 2 flying targets, in which the service interval is 0.8s. The targets trajectories are drawn in orange and red. The trajectory of the quadrotor is represented by 6 ghost images separated by 0.3s. The green box is the pitching machine. The yellow box is the starting position of quadrotor planning.

component since it determines all the expected quadrotor states. This article aims to provide a lightweight solution for catching, which can also be referenced for other highly dynamic tasks.

Although there exists some work that finished catching task, the catching time and terminal state still need to be determined manually or through a large number of trials, which lacks autonomy and flexibility. At present, there is no catching method that is fully autonomous and can generate dynamically feasible trajectories in real time. Furthermore, existing work can only catch single target. We summarize the requirements of catching tasks for high-speed targets as follow (FLAF):

- **Formulistic:** Planning-with-decision problems are hard or even impossible to explicitly formulate, which directly leads to the over simplification of planning-with-decision problems in previous work. Proper formulation is a powerful guarantee for optimal catching.
- **Lightweight:** Due to the errors in ego motion and target trajectory prediction, the drone needs high-frequency decision-making and re-planning, which requires lightweight method.
- **Adaptive:** When facing different flying targets, quadrotors need adaptively determine highly coupled catching time

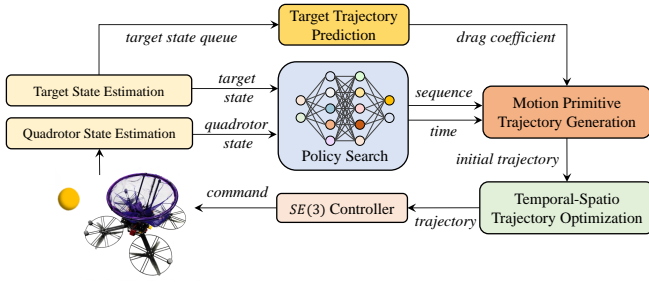


Fig. 2: The overview of Catch Planner. All parts run online.

and terminal position.

- **Flexible:** Quadrotors should be allowed to catch targets in any reasonable attitude and deviations from the ideal catching position, rather than fixed.

Unfortunately, it is difficult, even internally contradictory, to achieve these four aspects at the same time. Planning is usually decoupled with decision making in previous method. The over simplified decision making problem does not fully account for more refined trajectory planning, which results in the gap between planning and decision making. On the other hand, an optimal planning-with-decision method will iterate over all possible solutions and select the nearly optimal one rather than stop at a feasible solution. However, higher optimality comes from sophisticated formulation and more iterations or trials in the solution space, which significantly increases computation cost. Then, adaptability requires the joint optimization of coupled catching time and terminal position, which makes the problem non convex and challenging to find a solution. The introduction of flexibility further increases the difficulty of problem solving. In fact, only satisfying some basic requirements such as safety and feasibility while minimizing time and maximizing smoothness is already a difficult problem [7]. That is why most works are unable to take into account the above FLAF requirements at the same time.

In this paper, we propose a systematic scheme called Catch Planner to meet FLAF demands and use table tennis ball as targets in our catching experiments. The Catch Planner consists of Decision-making, Motion Primitive Trajectory Generation, Trajectory Optimization and Target Motion Perception modules, as shown in Fig. 2. We propose a deep reinforcement learning (DRL) based policy search method to solve the sequential decision making problem that is hard to formulate. In addition, we build simulation environment which decouples dynamics and physics to greatly reduce training computation consumption. (see Sec. IV for more details). Furthermore, the policy search results are used to generate control effort optimal motion primitive trajectory (see Sec. V-B for more details). Finally, we adopt MINCO trajectory class [29] to conduct trajectory re-parameterization and optimization. To make the catching adaptive, we propose a differentiable target trajectory model with online iterative correction (see Sec. V-A for more details). Based on the differentiable target trajectory representation, we jointly optimize highly coupled terminal states and catching time and propose a lightweight terminal constraint transcription method enabling the quadrotor to catch targets

at any reasonable attitude and position bias. Benefiting from sparse parametric optimization in MINCO and our constraint elimination and transcription approach (see Sec. VI for more details), FLAF requirements are satisfied. Eventually, the robustness and scalability are verified by extensive experiments in real world and simulation.

We summarize the contributions of our proposed Catch Planner as follows.

- A learning based sequential decision-making method and a self-supervised neural network policies training method are proposed for catching targets.
- We propose a terminal-flexible spatio-temporal trajectory optimization method which jointly optimize highly coupled terminal state and catching time, and trade off dynamic feasibility, control effort and safety.
- Catch Planner provides a new paradigm for merging learning and planning. The effectiveness is verified in extensive simulations and real-world experiments for catching.

## II. RELATED WORK

There are few researches on the catching task, especially for planning-with-decision. Most existing methods treat target catching as a fixed state-to-state motion planning problem. [1] proposes a closed-form solution to generate motion primitives for catching. This method is efficient, but the catching height must be determined manually or through trials. Furthermore, the dynamic feasibility of the trajectory is not considered while planning. [9] designs a controller to track the trajectory using the method from [1] with high following accuracy. [8] proposes a three-dimensional optimal terminal velocity control guidance for multicopter intercepting maneuvering drone with equal maneuverability level. This low-order planning leads to unsmooth trajectory. [5] shows two quadcopters cooperatively juggling a ball back-and-forth. The trajectory is calculated under small-angle assumption, but it does not take actuator saturation into account. A target prediction method is also proposed in [5] by integrating forward the current position and velocity. All the above planning method artificially fix the catching time and position, leading to reduced catching flexibility. In fact, coupled catching terminal and time make it difficult to jointly optimize the trajectory. Our work well overcome this difficulty. We also provide a method to make the quadrotor attitude and position offset flexible under the premise of successful catching.

There are also some catching works that tend to obtain complex decision variables, such as time and sequence. Although the sequential decision making problem can be modeled by introducing integer variables, it will cause a second-level computational burden [10] [11], which is intolerable for the catching task. The arrival of DRL method on robotics tasks [12] [13] [14] brings hope to solve the problem online. DRL has the power of improving the policy when the agent is constantly interacting with the environment by trial and error. However, most successful cases appear in simulation and games [15] rather than in reality. For catching task, [16] proposes an end-to-end method of visual reaction in the



#### IV. LEARNING-BASED SEQUENTIAL DECISION MAKING

In this section, we introduce the decision making framework and explain core terms design including rewards design, observation representation, action representation and invalid action masking in details. At the end we present the training strategy and platform.

##### A. Learning Neural Network Policies

1) *Decision Making Framework*: In our task, the decision making policy receives current quadrotor position, quadrotor attitude, quadrotor velocity, targets position and targets velocity as inputs, and outputs predicted time variables for catching each target. The decision making policy is trained using Proximal Policy Optimization (PPO) [25], which demonstrates impressive performance for continuous tasks. Our main objective is to update policy search network parameters  $\theta$  by maximizing the following:

$$\mathcal{J}_{DM}(\theta) = \mathbb{E}_t[\min(\frac{\pi_{\theta}(a_t|s_t)}{\pi_{\theta_{old}}(a_t|s_t)}\hat{A}_t, \text{clip}(\frac{\pi_{\theta}(a_t|s_t)}{\pi_{\theta_{old}}(a_t|s_t)}, 1 - \epsilon, 1 + \epsilon)\hat{A}_t)], \quad (5)$$

where  $\theta_{old}$  and  $\theta$  are the policy parameters before and after the update respectively,  $\hat{A}_t$  is an estimator of advantage function at time step  $t$  and  $\epsilon$  is a hyperparameter.

2) *State Representation*: The following components which are essential and minimalistic to represent states are used:

$$\mathbf{s}_t = [p_d(t), q_d(t), p_d^{(1)}(t), p_t(t), p_t^{(1)}(t)], \quad (6)$$

where  $p_d(t)$ ,  $q_d(t)$ ,  $p_d^{(1)}(t)$ ,  $p_t(t)$ ,  $p_t^{(1)}(t)$  stand for the quadrotor's position, attitude represented by quaternion, velocity and targets' position and velocity at time step  $t$ , respectively.

3) *Action Representation*: In our case, the decision-making time and sequence results are used in trajectory generation. To achieve this goal, we define the action  $\mathbf{a}_t$  to be predicted catching time sequence, which can be written as:

$$\pi_{\theta}(\mathbf{s}_t) = \mathbf{a}_t = \mathcal{T}_p, \quad (7a)$$

$$\pi_{\theta}(\mathbf{s}_t) \sim \mathcal{N}(\mu_t, \sigma_t), \quad (7b)$$

where  $\theta$  means the network parameters for policy search,  $\mathcal{T}_p$  represents predicted catching time sequence and each element of the sequence shows the predicted catching time for each target,  $\mathcal{N}$  is a multivariate Gaussian density function,  $\mu_t$  and  $\sigma_t$  are the mean and variance of the Gaussian distribution respectively.

4) *Reward Design*: In order to make the quadrotor catch as more targets as possible while flying smoothly and agilely, we design the reward signal which takes both caught targets amount, trajectory cost, optimized time and sequence into consideration at the same time. The reward signal  $\mathbf{r}_t$  is calculated by:

$$\mathbf{r}_t = \lambda_n(e^{n(t)-N} - e^{-N}) - \lambda_c \ln(\mathcal{J}) - \lambda_t \|\mathcal{T}_p - \mathcal{T}_o\|_2, \quad (8)$$

where  $n(t)$  suggests caught targets amount at time step  $t$ ,  $N$  represents total targets amount,  $\mathcal{J}$  indicates trajectory cost at time step  $t$ ,  $\lambda_n$ ,  $\lambda_c$  and  $\lambda_t$  are catching reward coefficient,

trajectory cost punishment coefficient and time punishment coefficient respectively and  $\|\mathcal{T}_p - \mathcal{T}_o\|_2$  means the L2 norm between predicted catching time sequence and optimized catching time sequence.

5) *Invalid Action Masking*: An action sampled directly from the whole action space can be typically invalid because time variable ranges from 0 to infinity. Invalid action masking is an applicable solution to deal with such problems. In our task, we firstly limit each time variable to the range from 0 to  $t_{max}$ , where  $t_{max}$  demonstrates maximum flying time of targets. Furthermore, it is also hard for quadrotor to catch targets within a surprisingly short time such as 0.1s. Therefore, we limit the predicted catching time within the range from  $t_{min}$  to  $t_{max}$ , where  $t_{min}$  denotes the minimum expected time for the quadrotor to catch targets.

##### B. Training Strategy and Platform

One hundred independent parallel training environments and agents are created and utilized to improve data collection speed, increase data quality and accelerate training speed. Our policy network is MLP with 2 hidden layers of 64 units and ReLU activation function, which is lightweight to run on real drone.

To speed up the self-supervised neural network policies training, we decouple physics environment and simulation environment from planning module. We define the process including targets states random initialization, quadrotor states random initialization, targets throwing, decision making, motion planning and targets catching as one step. After decision making, trajectory generation and optimization, we can directly obtain the catching result and trajectory cost by calculating the trajectory terminal state and target motion instead of executing the whole trajectory, which offers great improvement on training speed.

#### V. MOTION PRIMITIVE TRAJECTORY GENERATION

In this section, the purpose is to find a trajectory that is closer to the optimal trajectory, considering requirements for catching. First, we introduce the analytic expression method of target trajectory prediction, in which the expression are optimized by online iteration. Then we introduce the method of control effort cost minimum trajectory generation, which uses the results of decision making module as input.

##### A. Target Trajectory Prediction

Catching task needs accurate target state estimation and trajectory prediction. Eq. 2 shows that  $\dot{s}_b$  brings nonlinear effects for ball flying dynamics model, which is unacceptable for trajectory optimization. [26] proposed a simplified linear target model and trained a parameter identification neural network offline model to obtain  $K_D$ . We extend this model to online. Ball's linear equation of motion  $s_b(t)$  can be expressed as

$$s(t) = s_0 - \frac{\dot{s}_0 + \frac{g}{K_D}}{K_D} e^{-K_D t} - \frac{g}{K_D} t, \quad (9a)$$



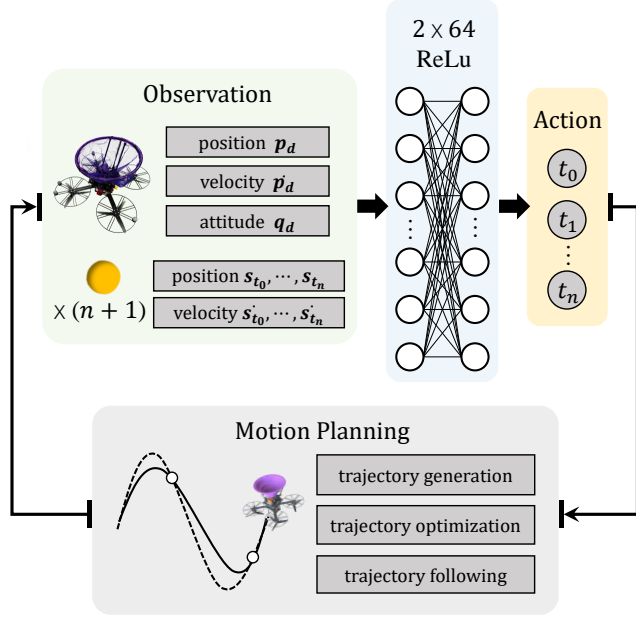


Fig. 4: The overview of the learning based sequential decision making.

where  $g$  and  $K_D$  are decoupled in  $\mathbf{e}$ ,  $s_0$  is the the initial ball's position each update. Note that Eq. 9 is continuously differentiable, so it is easy to obtain the gradient  $\partial s_b / \partial c_i$  and  $\partial s_b / \partial T_i$ . Then the extended kalman filter [27] (EKF) is used to optimize the observation value. The state transformation function is presented as

$$\begin{bmatrix} \mathbf{s}_{b_i}^t \\ \mathbf{v}_{b_i}^t \end{bmatrix} = \begin{bmatrix} \mathbf{I}_{3 \times 3} & \mathbf{I}_{3 \times 3} \Delta t \\ \mathbf{0} & \mathbf{I}_{3 \times 3} e^{-K_i \Delta t} \end{bmatrix} \begin{bmatrix} \mathbf{s}_{b_i}^{t-1} \\ \mathbf{v}_{b_i}^{t-1} \end{bmatrix} + \begin{bmatrix} \mathbf{0} \\ 1 \end{bmatrix} \frac{g(e^{-K_i \Delta t} - 1)}{K_i}, \quad (10)$$

where  $i \in \{x, y, z\}$ ,  $[\mathbf{s}_{b_i}^t \ \mathbf{v}_{b_i}^t]$  represent the target state at the moment  $t$ . Kalman state estimate at  $t$  can be expressed by

$$\mathbf{s}_b^{cor} = \mathbf{s}_b^t + K_a(Z - \mathbf{H}\mathbf{s}_b^t), \quad (11)$$

where the observation matrix  $\mathbf{H} = [\mathbf{I}_{3 \times 3} \ \mathbf{0}_{3 \times 3}]^T$ ,  $K_a$  denotes kalman gain.  $Z$  denotes the motion capture observation. To make  $K_D$  more accurate, we use nonlinear least squares method [28] to optimize  $K_D$  online. The cost function is constructed as

$$\mathcal{J}_{K_D} = \sum_i^{i+n} (\mathbf{s}_b^{cor} - \mathbf{s}_b)^2, \quad (12)$$

where  $n$  represents the number of states used for optimization in continuous time. The goal is to minimize it, which is efficiently solved by Ceres Solver<sup>1</sup>.

### B. Motion Primitive trajectory generation

The motion primitive generator [1] is considered as an efficient method to plan a state-to-state trajectory, which is

<sup>1</sup><https://github.com/ceres-solver/ceres-solver>

closed-form. We use it as the front end of trajectory optimization. Consider an  $m$ -dimensional trajectory whose  $i$ -th piece is denoted by a  $N = 2s - 1$  degree polynomial:

$$p(t) = \mathbf{c}_i^T \beta(t), t \in [0, T_i], \quad (13)$$

where  $\mathbf{c}_i \in \mathbb{R}^{2s \times m}$  is the coefficient matrix,  $T_i$  is obtained from the policy searching,  $\beta(t) = (1, t, \dots, t^N)^T$  is the natural basis.

Following [1], we consider the motion of the quadrotor in terms of the jerk  $s = 3$ , allowing the system to be considered as a triple integrator in each axis, and minimize the cost function

$$\mathcal{J}_{MP} = \frac{1}{T} \int_T^0 \|p^{(3)}(t)\|^2 dt, \quad (14)$$

where  $T$  is from decision-making module. Just like [1], we use Pontryagin's minimum principle [27] to generate the optimal state trajectory by introducing the costate  $\lambda_m = (\lambda_1, \lambda_2, \lambda_3)$  and defining the Hamiltonian function  $H(s, j, \lambda_m)$  as

$$H(s, j, \lambda_m) = \frac{1}{T} j^2 + \lambda_m^T f_s(s, j) = \frac{1}{T} j^2 + \lambda_1 v + \lambda_2 a + \lambda_3 j, \quad (15a)$$

$$\dot{\lambda}_m = \nabla H(s^*, j^*, \lambda_m) = (0, -\lambda_1, -\lambda_2), \quad (15b)$$

where  $j^*$  and  $s^*$  represent the optimal input and state. The cost value can be calculated as

$$\mathcal{J}_{MP} = \gamma^2 + \beta\gamma T + \frac{1}{3}\beta^2 T^2 + \frac{1}{3}\alpha\gamma T^2 + \frac{1}{4}\alpha\beta T^3 + \frac{1}{20}\alpha^2 T^4, \quad (16)$$

where  $\alpha, \beta$  and  $\gamma$  are constants. They are explicitly calculated according to current state of the quadrotor  $s(0)$  and final state  $s(T)$ , which is determined by Eq. 9 and  $T$  from the policy search. For more details, please see [1]. Then we can get the initial trajectory  $p_0(t)$ .

## VI. TERMINAL-FLEXIBLE TEMPORAL-SPATIO TRAJECTORY OPTIMIZATION FOR CATHING

In this section, we summarize the proposed trajectory optimization method for catching, which jointly optimizes all the requirements in the planning module. The problem form can be efficiently transformed from Eq. 3 into a new form of unconstrained nonlinear programming. The generated trajectory  $p_0(t)$  is used to generate the initial values. Moreover, a lightweight terminal constraint transcription method is proposed to make catching more flexible.

### A. MINCO Trajectory Class

We adopt  $\mathfrak{T}_{\text{MINCO}}$  for trajectory representation, which is a **minimum control** (MINCO) [29] polynomial trajectory class, defined as

$$\mathfrak{T}_{\text{MINCO}} = \left\{ p(t) : [0, T] \mapsto \mathbb{R}^m \mid \mathbf{c} = \mathcal{M}(\mathbf{q}, \mathbf{T}), \right. \\ \left. \mathbf{q} \in \mathbb{R}^{m(M-1)}, \mathbf{T} \in \mathbb{R}_{>0}^M \right\}, \quad (17)$$

where an  $m$ -dimensional trajectory  $p(t)$  is represented by a piece-wise polynomial of  $M$  pieces and  $N = 2s - 1$

degree. In this paper, we use  $s = 4$  for minimum snap for enough freedom of trajectory. All trajectories in  $\mathfrak{T}_{\text{MINCO}}$  have compact parameterization by only the intermediate way-point vector  $\mathbf{q}$  and time vector  $\mathbf{T}$  via the linear-complexity formulation  $\mathbf{c} = \mathcal{M}(\mathbf{q}, \mathbf{T})$ . Furthermore, any cost function  $\mathcal{J}(\mathbf{q}, \mathbf{T}) = F(\mathcal{M}(\mathbf{q}, \mathbf{T}), \mathbf{T})$ . The mapping also gives a linear-complexity way to compute  $\partial\mathcal{J}/\partial\mathbf{q}$  and  $\partial\mathcal{J}/\partial\mathbf{T}$  from  $\partial F/\partial\mathbf{q}$  and  $\partial F/\partial\mathbf{T}$ . After that, a high-level optimizer is able to optimize the objective efficiently.

### B. Trajectory Joint Optimization

Considering all described requirements in Eq. 3, we adopt the compact parameterization of  $\mathfrak{T}_{\text{MINCO}}$ , temporal constraint elimination, and constraint penalty to transform trajectories generation problem into an unconstrained nonlinear optimization problem:

$$\min_{\mathbf{c}, \mathbf{T}} \sum_{i=1} \mathcal{J}_e + \lambda \cdot [\mathcal{J}_t, \mathcal{J}_p, \mathcal{J}_\theta, \mathcal{J}_v, \mathcal{J}_\omega, \mathcal{J}_f, \mathcal{J}_g], \quad (18)$$

where  $i$  is the number of the targets,  $\lambda$  is the weight vector.

1) *Control Effort  $\mathcal{J}_e$* : The control cost is the same as Eq. 3a. Then the gradients  $\partial\mathcal{J}_e/\partial\mathbf{c}$  and  $\partial\mathcal{J}_e/\partial\mathbf{T}$  are evaluated as

$$\mathcal{J}_e = \int_0^T \|p_i^{(4)}(t)\|^2 dt, \quad (19a)$$

$$\frac{\partial\mathcal{J}_e}{\partial c_i} = 2 \left( \int_0^{T_i} \beta^{(3)}(t) \beta^{(3)}(t)^T dt \right) c_i, \quad (19b)$$

$$\frac{\partial\mathcal{J}_e}{\partial T_i} = c_i^T \beta^{(3)}(T_i) \beta^{(3)}(T_i)^T c_i, \quad (19c)$$

2) *Temporal Constraint Elimination  $\mathcal{J}_t$* : In order to catch more targets, shorter total time is eagerly expected. We minimize the total time just like Eq. 3a.

$$\mathcal{J}_t = \rho T_i. \quad (20)$$

Meanwhile, Eq. 3b, which requires the strict positiveness of each entry in  $\mathbf{T}$ , does harm to the optimization process. We eliminate it by explicit diffeomorphism in Euclidean spaces as  $T_i = e^{t_i}$ . Therefore,  $t_i \in \mathbb{R}$  instead of  $T_i \in \mathbb{R}_+$  becomes the new optimal variable. The gradient is calculated by

$$\frac{\partial\mathcal{J}_t}{\partial c_i} = 0, \quad \frac{\partial\mathcal{J}_t}{\partial t_i} = \frac{\partial\mathcal{J}_t}{\partial T_i} e^{t_i}. \quad (21)$$

3) *Flexible Terminal Transformation  $\mathcal{J}_p, \mathcal{J}_\theta$* : Since the flat-output [30] characteristics of quadrotor, the terminal state can be determined by  $p_i^{(s-1)}(T_i)$ . Eq. 3f shows the ideal situation for catching. Such a strict restriction is obviously not in line with reality. The quadrotor shall be able to catch the ball at any position in the net with any attitude, as shown in the Fig. 3. We relax the constraints by designing a penalty function

$$\mathcal{J}_p = \mathcal{L}_\varepsilon[\mathcal{G}_p(t)], \quad \mathcal{G}_p(t) = \|p - s_b - \bar{\mathbf{l}}_{\mathbf{z}d}\|. \quad (22)$$

In order to make the catching position flexible while inside the net, we design a smooth and continuous logistic function

$$\mathcal{L}_\varepsilon[x] = \begin{cases} 0, & x \leq 0, \\ x^3, & 0 < x \leq \varepsilon, \\ \varepsilon^3 + (x - \varepsilon)^2 x / \varepsilon^4, & x > \varepsilon, \end{cases} \quad (23)$$

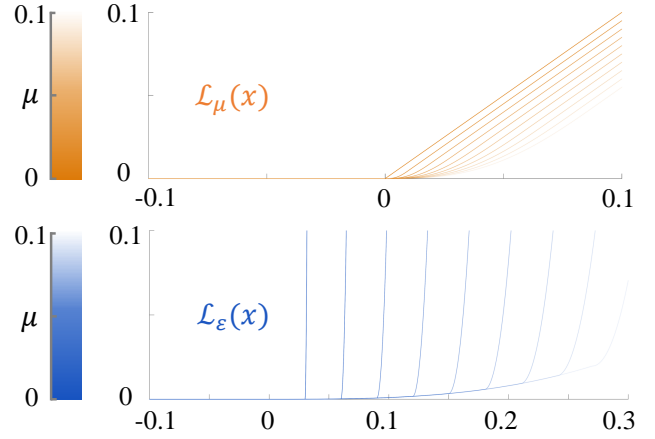


Fig. 5: The logistic function.

where the gradient changes smoothly when  $0 < x \leq \varepsilon$ , while drastic when  $x > \varepsilon$ , meaning stronger penalties for violating constraints. Then the gradient

$$\frac{\partial\mathcal{J}_p}{\partial c_i} = \frac{\partial\mathcal{J}_p}{\partial\mathcal{G}_p} \frac{\partial\mathcal{G}_p}{\partial c_i} = 0, \quad \frac{\partial\mathcal{J}_p}{\partial T_i} = \frac{\partial\mathcal{J}_p}{\partial\mathcal{G}_p} \frac{\partial\mathcal{G}_p}{\partial s_b} \frac{\partial s_b}{\partial T_i}. \quad (24)$$

It is worth noting that each item can be calculated by Eq. 9, Eq. 22 and Eq. 23.

The angle constraint Eq. 3g requires that the quadrotor's terminal attitude  $\mathbf{z}_d$  and the moving direction of the flying target are kept within a safe range. This constraint is translated into the following penalty function.

$$\mathcal{G}_\theta(t) = \cos \theta_{safe} - \frac{\dot{s}_b \cdot \mathbf{z}_d}{\|\dot{s}_b\| \|\mathbf{z}_d\|}, \quad \mathcal{J}_\theta = \mathcal{L}_\varepsilon[\mathcal{G}_\theta(t)]. \quad (25)$$

And the gradient can be calculated just like Eq. 24.

4) *Continuous-Time Constraints  $\mathcal{J}_v, \mathcal{J}_\omega, \mathcal{J}_f, \mathcal{J}_g$* :  $\mathfrak{T}_{\text{MINCO}}$  can be freely deformed to meet the continuous-time constraints  $\mathcal{G}$ . However, enforcing  $\mathcal{G}$  over the entire trajectory involves infinitely many inequalities that cannot be solved by constrained optimization. Inspired by [29], We transform  $\mathcal{G}$  into finite inequality constraints using integral of constraint violations.

$$\mathcal{I}_i^* = \frac{T_i}{\kappa} \sum_{j=0}^{\kappa_i} \bar{\omega}_j \mathcal{G}_*(\frac{j}{\kappa} T_i), \quad \mathcal{J}_* = \sum_{i=1}^M \mathcal{I}_i^*, \quad (26a)$$

$$\frac{\partial\mathcal{J}_*}{\partial c_i} = \frac{\partial\mathcal{I}_i^*}{\partial\mathcal{G}_*} \frac{\partial\mathcal{G}_*}{\partial c_i}, \quad \frac{\partial\mathcal{J}_*}{\partial T_i} = \frac{\mathcal{I}_i^*}{T_i} + \frac{j}{\kappa} \frac{\partial\mathcal{I}_i^*}{\partial\mathcal{G}_*} \frac{\partial\mathcal{G}_*}{\partial t}, \quad (26b)$$

where integer  $\kappa$  controls the relative resolution of quadrature.  $(\bar{\omega}_0, \bar{\omega}_1, \dots, \bar{\omega}_{\kappa_i-1}, \bar{\omega}_{\kappa_i}) = (1/2, 1, \dots, 1, 1/2)$  are the quadrature coefficients following the trapezoidal rule [31].  $i = (1, 2, \dots, N)$  denotes the  $i$ -th piece and  $j = (1, 2, \dots, \kappa)$ .

a) *Actuator Constraints*: Inspired by [32], velocity  $p_i^{(1)}(t)$ , body rate  $\omega$  and thrust  $\tau$  of Eq. 3d can be constrained by constructing such a penalty function as follow, and the penalty gradients are calculated by

$$\mathcal{G}_D(t) = \mathcal{L}_\mu[\|D(t)\|^2 - D_{max}^2], \quad D = p_i^{(1)}(t), \omega, \tau, \quad (27a)$$

$$\mathcal{L}_\mu[x] = \begin{cases} 0, & x \leq 0, \\ (\mu - x/2)(x/\mu)^3, & 0 < x \leq \mu, \\ x - \mu/2, & x > \mu. \end{cases} \quad (27b)$$

$$\frac{\partial \mathcal{G}_D}{\partial c_i} = 2\beta_i^{(n)}(t)p_i^{(n)}(t)^T \frac{\mathcal{L}_\mu}{\partial x}, \quad (27c)$$

$$\frac{\partial \mathcal{G}_D}{\partial T_i} = 2\beta_i^{(n)}(t)c_i p^{(n)}(t) \frac{\mathcal{L}_\mu}{\partial x}. \quad (27d)$$

*b) Safety Constraints:* The safety constraint Eq. 3e avoiding the collision with ground can be transformed as such a penalty function [3] as follow

$$\mathcal{G}_g(t) = \mathcal{L}_\mu [z_{min}^2 - \|e_3^T p(t)\|^2]. \quad (28)$$

And the gradient is calculated just like Eq. 27.

Summarizing the above strategies, the constraints of the Eq. 3 are unified to the same unconstrained cost function Eq. 18. The requirements can be trade off by adjusting the weight vector  $\lambda$ . We set initial value according to  $p_0(t)$  in Section V-B by calculating each intermediate waypoint position using the uniform time from decision making module. The problem is then efficiently solved by the L-BFGS [33] whose solver is open source<sup>2</sup>.

## VII. EXPERIMENTS

We design real scenes and simulated scenes to verify the robustness and extensibility of Catch Planner, and compare with the benchmark.

### A. Real-world Experiments

*1) Experiments Platform:* We design a quadrotor with a net attached above the center of mass, shown as Fig. 6c. An NUC-11TNHI5 is used as the onboard computer and all programs run on Intel I5-1135G7 CPU at 2.4GHz. Motion Primitive Planner (MPP) [1] is as the benchmark, which runs on the same computer. A  $18m \times 9m \times 5m$  motion capture gym with 22 Vicon cameras is used as the experimental site, shown in Fig. 6a. A pitching machine with two driven rubber wheels is used for throwing balls, shown as Fig. 6d. The state estimation of the quadrotor is given by an EKF of the pose from Vicon cameras and the IMU data from a PX4 Autopilot. We adopt the  $SE(3)$  cascade PID controller using Hopf fibration [34] to avoid singularities and align the attitude calculation of planning and control. Control command is calculated from the trajectory by using differential flatness output model [30].

The target throwing position is set at  $(4, 0, 0.8)$  under world coordinate. Because the throwing is random, the ball's landing position is within  $2m \times 0.8m$  at height  $0m$ , shown in Fig. 6b. Due to the height limitation, the balls only fly below  $4.2m$ , which means that the flight time of the ball does not exceed  $1.9s$ . In fact, in our experiment, the sensing data is considered stable and used only after the balls are thrown more than  $2m$ . After the first target motion model updated, the state of the ball is output after the ball exceeds the height of  $2.8m$ . In this case, the whole flight time of each target does not exceed  $1.6s$ .

*2) Experimental Results:* We check the dynamic, safety and catching constraints of the desired trajectory to ensure that the calculated trajectory is executable. If the trajectory passes the check, the decision and planning are considered successful. If the ball falls into the net, it will be regarded as a successful catching. In addition, we propose the optimal time ratio (OTR) to measure the gap between decision results and optimal results. The MPP has no OTR because it has no decision-making ability. The OTR is defined as follows:

$$OTR = \frac{1}{n} \sum \frac{|T_o - T_p|}{T_o}, \quad (29)$$

which measures the proximity of  $n$  output of the decision-making module  $T_p \in \mathcal{T}_p$  and optimized time  $T_o \in \mathcal{T}_o$ . Obviously, the closer the decision result is to the optimal result, the smaller OTR is. It also provides a pattern for measuring the ability of decision making under similar planning-with-decision frameworks.

We carry out 50 experiments respectively for Catch Planner and MPP [1]. Like [1], we set the terminal catching height below  $2m$ . The terminal velocity and acceleration are sampled, and the trajectory with the lowest cost is finally adopted. Table I summarizes the experimental results. It can be seen that the success rate of Catch Planner is far greater than that of MPP. Due to the gap between ideal and reality, the success rate of catching will never be higher than the success rate of planning, which is caused by various errors.

TABLE I: Success Rate and Optimal Time Ratio

	Planning Success Rate	Catching Success Rate	OTR
Catch Planner	96%	64%	0.092
MPP [1]	14%	8%	-

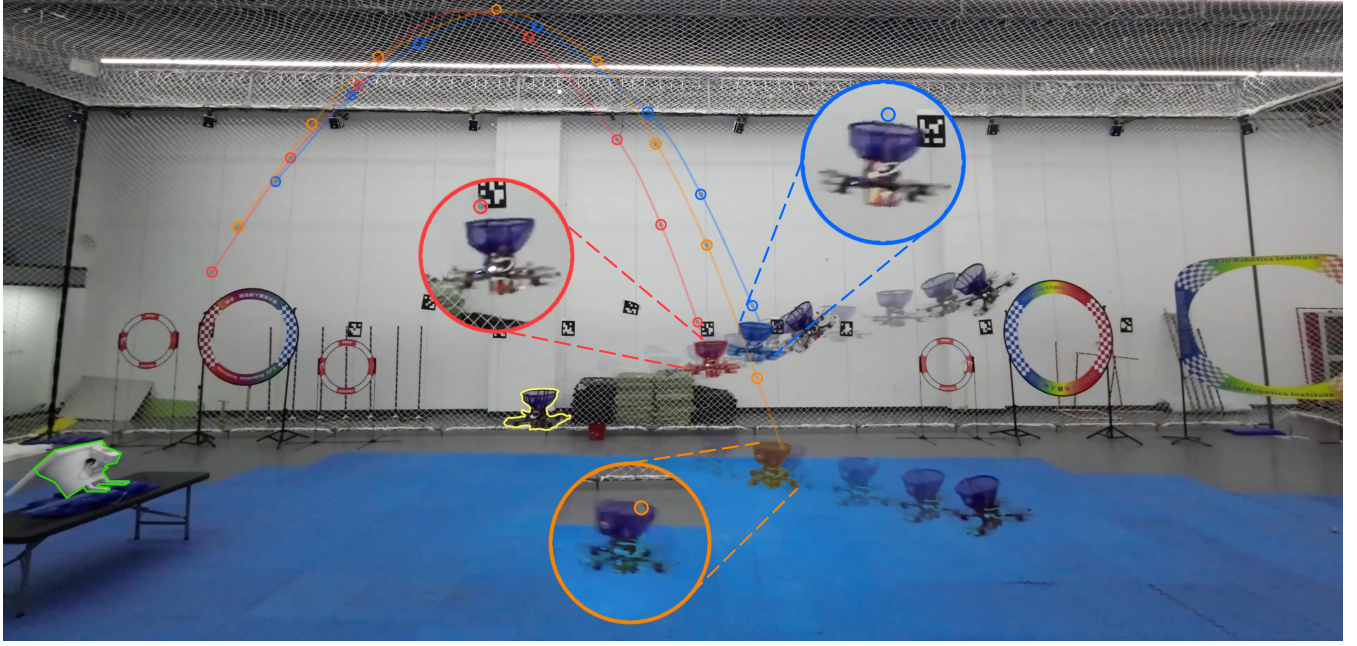
Three consecutive successful catch cases are selected to analyze the dynamics. We only visualize the real data of the quadrotor during moving, not including hovering. Fig. 6e-g show that the planned trajectory can effectively constrain the velocity, angular velocity and thrust. Fig. 6h shows that the planned trajectory is smooth enough, even jerk.

We compare Catch Planner with the state-of-the-art catching method MPP. The logged bag of the first catching in Fig. 6 is used to simulate the same throwing. The catching time is set to be the same, which means the same state of caught target. The desired trajectory of MPP is shown in the Fig. 7. It can be seen that ignoring the dynamic feasibility and safety of the benchmark leads to some actuator's command exceeding the limit, which often appears in the 50 experiments.

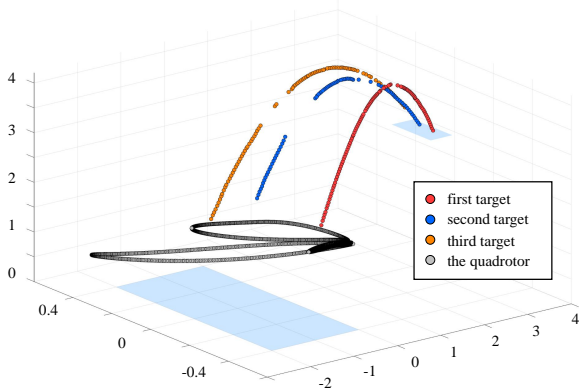
Our method can also catch multiple flying balls, which benefits from the real-time decision making ability. Although it is within the  $4.2m$  height limit, the quadrotor still shows the ability to catch two targets flying together in the air, as shown in Fig. 1.

The characteristics of Catch Planner and MPP are summarized as the Table II. MPP does not have high-level decision

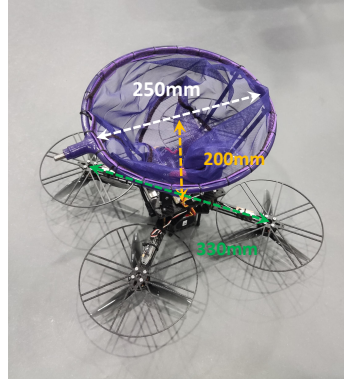
<sup>2</sup><https://github.com/ZJU-FAST-Lab/LBFGS-Lite>



(a) The process of the quadrotor catching triple targets continuously



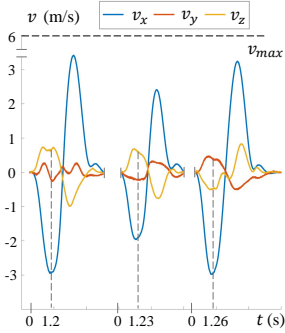
(b) Position map of ball catching process



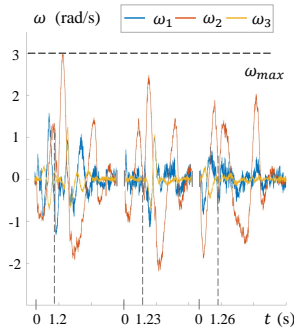
(c) The quadrotor



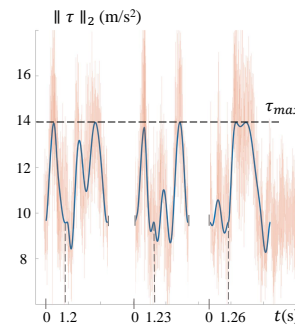
(d) The pitching machine



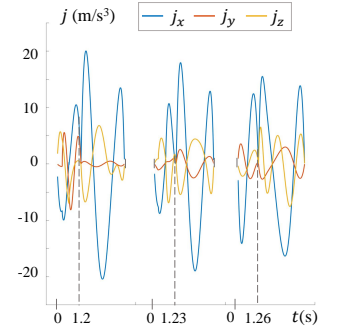
(e) Velocity



(f) Body Rate



(g) Thrust



(h) Jerk

Fig. 6: Experimental platform and results. (a) shows the process of catching triple targets. The time from each target thrown to hitting the ground (if not caught) is less than 1.9s. The time left for the quadrotor response is less than 1.6s. The catching time is less than 1.3s. The motion trajectories of three targets are represented by red, blue and orange respectively. Local images are magnified to see the moment of catching the targets clearly. The trajectories of the quadrotor are represented by ghost images. The green box is the pitching machine. The yellow box is the starting position of quadrotor planning. (b) shows the positions of the quadrotor and the targets moving measured by Vicon cameras. The translucent rectangle is the area where the ball is measured for the first time and the landing position. (c) shows the quadrotor designed by ourselves. The diameter of catching net is 250mm, and the diagonal propeller distance of the quadrotor is 330mm. The distance between the hoop plane and the propeller plane is 200mm. (d) shows the pitching machine. The ball is pushed to the tee by the wave wheel, and the ball is squeezed and launched by two rubber wheels driven by brushless motors. (e) shows the quadrotor velocity from an EKF. (f) shows the quadrotor angular rate measured by the IMU. Due to the vibration of the rack, the curve has a small jitter, which is a normal phenomenon. (g) shows the thrust. The orange translucent lines are the measured value with noise, and blue is the expected command. (h) shows the desired jerk.



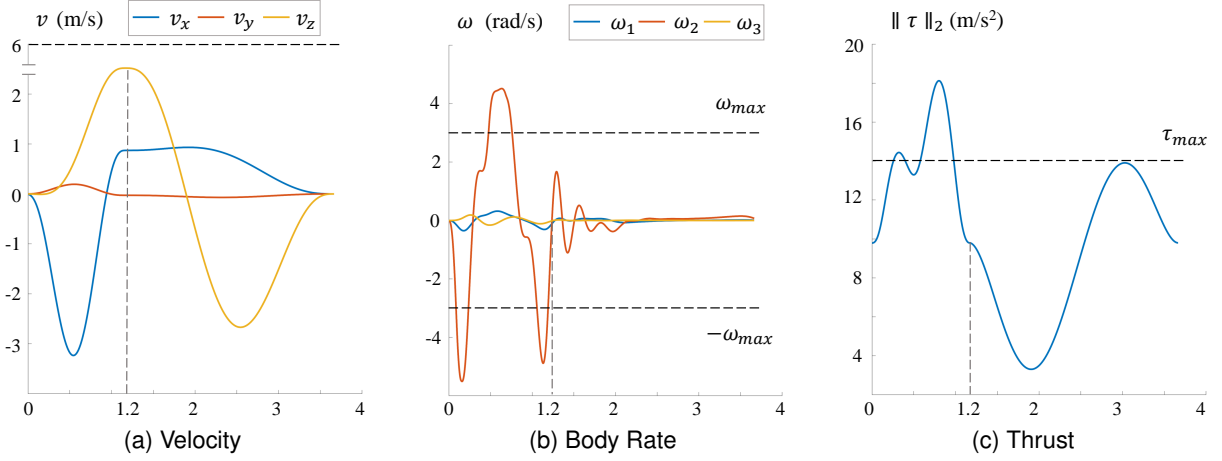


Fig. 7: The MPP's planning dynamic curve.

TABLE II: Characteristics comparison

	Catch Planner	Benchmark's
Decision-making Ability	<b>Autonomous</b>	Manual
Time & Terminal State	<b>Optimize</b>	Fix
Dynamic Feasibility	<b>Optimize</b>	Check
Crash Safety	<b>Optimize</b>	Check
Computing Consumption	9 ms	<b>0.149 ms</b>

trajectory types. Compared with real experiments, simulation scenarios effectively eliminate the target prediction error, sensing error, control error and communication delay in the real environment, so that we can focus on verifying the effectiveness of planning-with-decision methods. Thanks to the economy of simulation, we test 1000 experiments for each scenario in short time. The different trajectories types of the targets are as follow:

a) *Parabola*: This simulation to throw 2 targets is highly consistent with the real experimental scene, except that the target is free from height limitation and wind resistance. The change of position from initial position  $p_0$  can be expressed by acceleration  $a$  and velocity  $v_{pa}$  motion trajectory as  $p_{pa}(t) = 1/2at^2 + v_{pa}t + p_0$ ,  $t < 2$ .

b) *Harmonic*: 2 targets move at the speed  $v_{ha}$  in the shape of harmonic, expressed as  $p_{ha}(t) = \sin(v_{ha}t) + p_0$ ,  $t < 7$ .

c) *Triangle*: 3 diagonally moving objects move and form an equilateral triangle. For the  $i$ -th and  $j$ -th targets, the position can be calculated as  $p_{tr}(t) = v_{tr}t + p_0$ ,  $\langle v^i, v^j \rangle = 2/3\pi$  and  $v^i \neq v^j$  for  $\forall v^i, v^j$ ,  $t < 6$ .

d) *Hexagon*: The position of 6 targets flying in parallel at a constant velocity  $v_{he}$  can be expressed as  $p_{he}(t) = v_{he}t + p_0$ ,  $t < 10$ .

It is worth noting that the above trajectories are all on  $e_3$ . The target keeps constant velocity on  $e_1$  and  $e_2$ .

2) *Experimental Results*: In our simulation experiment, there is no target trajectory prediction and quadrotor control error. The success rate in Table III can reflect the ability of our method through thousands of experiments.

The results show that the catching difficulty increases as the targets amount increases and trajectory becomes more complex, which is due to the parameter random initialization in training and testing experiment.

Experience tells us that the success rate usually exceeds 80% when the OTR is below 0.3. Although it has not been proved by theory, it can be used as a reference for researchers.

The experimental results demonstrate the scalability of our method. In fact, the only requirement for using our method is that the motion of targets can be differentially analytically ex-

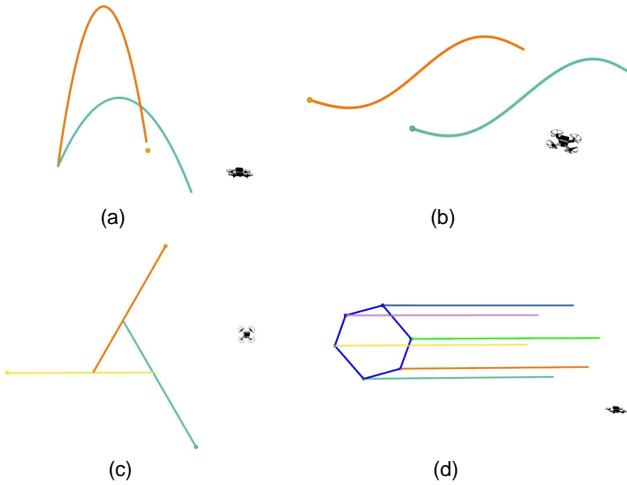


Fig. 8: The simulation scenarios. Multiple flight paths of the target are visualized as curves with multiple colors. (a) Parabola. (b) Harmonic. (c) Triangle. (d) Hexagon.

making ability, but relies on manual assignment. The state of the target is highly coupled with the time. This is not considered by MPP [1]. The dynamic feasibility and safety are also ignored during planning and only checked the end state. In addition, For computing consumption, although the calculated time of a single trajectory in [1] is far less than our method, 9ms is enough for the 100hz frequency of state estimation and control, while only 2ms is required for re-planning.

### B. Simulation Experiments

1) *Scene Simulation*: We design 4 scenarios to evaluate our planning-with-decision method according to different target

pressed. This condition can be easily achieved by establishing curve fitting or simplifying dynamic models.

TABLE III: Success Rate

	Parabola (1 target)	Parabola (2 targets)	Harmonic (2 targets)	Triangle (3 targets)	Hexagon (6 targets)
Success Rate	99.3%	98.2%	84.7%	99.7%	76.3%
OTR	0.052	0.119	0.234	0.126	0.458

## VIII. CONCLUSION

In this paper, we propose a novel planning-with-decision framework Catch Planner to catch high-speed moving targets when facing Formulative, Lightweight, Adaptive and Flexible requirements (FLAF). It integrates decision making, trajectory generation and optimization, and target trajectory prediction modules.

Under Catch Planner framework, the advantages of learning based and optimization based methods complement each other by the coupling of planning and decision making, meeting the Formulative need. We propose a policy search method based on DRL to solve the decision making problem, and propose a self-supervised neural network training method. Then, we propose a spatio-temporal optimal trajectory optimization method for optimal catching. Facing different flying targets, the coupling time and terminal position are jointly optimized to Adaptively catch, and a terminal constraint transformation method is proposed to make the catching Flexible. All the above are solved online with the calculation consumption does not exceed 10ms, which proves the Lightweight of the framework.

We conduct simulations and real experiments to verify the robustness of the proposed method. The real world planning success rate is 96%. The universality and scalability of the algorithm are verified by setting different target trajectories. Furthermore, this method has the potential to solve other highly dynamic problems.

## IX. ACKNOWLEDGMENT

The authors would like to thank Prof. H. Li and L. Xu for their helps in the establishment of experimental site.

## REFERENCES

- [1] M. W. Mueller, M. Hehn and R. D'Andrea, "A Computationally Efficient Motion Primitive for Quadcopter Trajectory Generation," in *IEEE Transactions on Robotics*, vol. 31, no. 6, pp. 1294-1310, Dec. 2015.
- [2] R. W. Beard, T. W. McLain, M. A. Goodrich and E. P. Anderson, "Coordinated target assignment and intercept for unmanned air vehicles," in *IEEE Transactions on Robotics and Automation*, vol. 18, no. 6, pp. 911-922, Dec. 2002.
- [3] Ji, Jialin, et al., "Real-Time Trajectory Planning for Aerial Perching," in *arXiv preprint*, arXiv:2203.01061 (2022).
- [4] R. Lal and P. Prabhakar, "Time-Optimal Multi-Quadrotor Trajectory Planning for Pesticide Spraying," in *2021 IEEE International Conference on Robotics and Automation (ICRA)*, 2021, pp. 7965-7971.
- [5] M. Müller, S. Lupashin and R. D'Andrea, "Quadcopter ball juggling," in *2011 IEEE/RSJ International Conference on Intelligent Robots and Systems (IROS)*, 2011, pp. 5113-5120.
- [6] Foeht P, Romero A, Scaramuzza D, "Time-optimal planning for quadrotor waypoint flight," in *Science Robotics*, 2021, 6(56): eab1221.
- [7] X. Zhou, Z. Wang, H. Ye, C. Xu and F. Gao, "EGO-Planner: An ESDF-Free Gradient-Based Local Planner for Quadrotors," in *IEEE Robotics and Automation Letters*, vol. 6, no. 2, pp. 478-485, April 2021
- [8] Tao H, Lin D, He S, et al., "Optimal terminal-velocity-control guidance for intercepting non-cooperative maneuvering quadcopter," in *Journal of Field Robotics*, 2022, 39(4): 457-472.
- [9] W. Dong, G. -Y. Gu, Ye Ding, X. Zhu and H. Ding, "Ball juggling with an under-actuated flying robot," in *2015 IEEE/RSJ International Conference on Intelligent Robots and Systems (IROS)*, 2015, pp. 68-73.
- [10] B. Landry, R. Deits, P. R. Florence and R. Tedrake, "Aggressive quadrotor flight through cluttered environments using mixed integer programming," in *2016 IEEE International Conference on Robotics and Automation (ICRA)*, 2016, pp. 1469-1475.
- [11] R. Deits and R. Tedrake, "Efficient mixed-integer planning for UAVs in cluttered environments," in *2015 IEEE International Conference on Robotics and Automation (ICRA)*, 2015, pp. 42-49.
- [12] Y. Song and D. Scaramuzza, "Learning High-Level Policies for Model Predictive Control," in *2020 IEEE/RSJ International Conference on Intelligent Robots and Systems (IROS)*, 2020, pp. 7629-7636.
- [13] R. Penicka, Y. Song, E. Kaufmann and D. Scaramuzza, "Learning Minimum-Time Flight in Cluttered Environments," in *IEEE Robotics and Automation Letters*, vol. 7, no. 3, pp. 7209-7216, July 2022.
- [14] Y. Song and D. Scaramuzza, "Policy Search for Model Predictive Control With Application to Agile Drone Flight," in *IEEE Transactions on Robotics*, vol. 38, no. 4, pp. 2114-2130, Aug. 2022.
- [15] Vinyals, O., Babuschkin, I., Czarnecki, W.M. et al., "Grandmaster level in StarCraft II using multi-agent reinforcement learning," in *Nature*, 575, 350-354 (2019).
- [16] K. -H. Zeng, R. Mottaghi, L. Weihs and A. Farhadi, "Visual Reaction: Learning to Play Catch With Your Drone," in *2020 IEEE/CVF Conference on Computer Vision and Pattern Recognition (CVPR)*, 2020, pp. 11570-11579.
- [17] R. Silva, F. S. Melo and M. Veloso, "Towards table tennis with a quadrotor autonomous learning robot and onboard vision," in *2015 IEEE/RSJ International Conference on Intelligent Robots and Systems (IROS)*, 2015, pp. 649-655.
- [18] X. Meng, X. Ding and P. Guo, "A Net-Launching Mechanism for UAV to Capture Aerial Moving Target," in *2018 IEEE International Conference on Mechatronics and Automation (ICMA)*, 2018, pp. 461-468.
- [19] P. Bouffard, A. Aswani and C. Tomlin, "Learning-based model predictive control on a quadrotor: Onboard implementation and experimental results," in *2012 IEEE International Conference on Robotics and Automation*, 2012, pp. 279-284.
- [20] Y. Stasinchuk et al., "A Multi-UAV System for Detection and Elimination of Multiple Targets," in *2021 IEEE International Conference on Robotics and Automation (ICRA)*, 2021, pp. 555-561.
- [21] K. Yang and Q. Quan, "An Autonomous Intercept Drone with Image-based Visual Servo," in *2020 IEEE International Conference on Robotics and Automation (ICRA)*, 2020, pp. 2230-2236.
- [22] K. Su, and S. Shen, "Catching a flying ball with a vision-based quadrotor," in *International Symposium on Experimental Robotics*. Springer, Cham, 2016:550-562.
- [23] M. W. Mueller and R. D'Andrea, "A model predictive controller for quadcopter state interception," in *2013 European Control Conference (ECC)*, 2013, pp. 1383-1389.
- [24] J. Nonomura, A. Nakashima and Y. Hayakawa, "Analysis of effects of rebounds and aerodynamics for trajectory of table tennis ball," in *Proceedings of SICE Annual Conference 2010*, 2010, pp. 1567-1572.
- [25] Schulman J, Wolski F, Dhariwal P, et al., "Proximal policy optimization algorithms," in *arXiv preprint arXiv:1707.06347*, 2017.
- [26] Zhang Y, Xiong R, Zhao Y, et al., "An adaptive trajectory prediction method for ping-pong robots," in *International conference on intelligent robotics and applications*. Springer, Berlin, Heidelberg, 2012: 448-459.
- [27] D. P. Bertsekas, *Dynamic Programming and Optimal Control*, Vol. I. Athena Scientific, 2005.
- [28] Levenberg, Kenneth, "A method for the solution of certain non-linear problems in least squares," in *Quarterly of applied mathematics*, 2.2 (1944): 164-168.
- [29] Z. Wang, X. Zhou, C. Xu and F. Gao, "Geometrically Constrained Trajectory Optimization for Multicopters," in *IEEE Transactions on Robotics*, vol. 38, no. 5, pp. 3259-3278, Oct. 2022.
- [30] D. Mellinger and V. Kumar, "Minimum snap trajectory generation and control for quadrotors," in *2011 IEEE International Conference on Robotics and Automation*, 2011, pp. 2520-2525.
- [31] Press, William H., et al., "Numerical recipes 3rd edition: The art of scientific computing," in *Cambridge university press*, 2007.

- [32] Wang, Zhepei, Chao Xu, and Fei Gao, "Robust Trajectory Planning for Spatial-Temporal Multi-Drone Coordination in Large Scenes," in *arXiv preprint*, arXiv:2109.08403 (2021).
- [33] D. C. Liu and J. Nocedal, "On the limited memory bfgs method for large scale optimization," in *Mathematical programming*, vol. 45, no. 1, pp. 503–528, 1989.
- [34] Watterson M, Kumar V, "Control of quadrotors using the hopf fibration on  $so(3)$ ," in *Robotics Research*. Springer, Cham, 2020: 199-215.